Eur. Phys. J. B **33**, 165–171 (2003)
DOI: 10.1140/epjb/e2003-00153-0

THE EUROPEAN PHYSICAL JOURNAL B

Effective nonlinear optical properties of shape distributed composite media

Lei Gao[1,2,a] and Yanyan Huang[2]

[1] CCAST (World Laboratory), PO Box 8730, Beijing 100080, PR China
[2] Department of Physics, Suzhou University, Suzhou 215006, PR China

Received 10 December 2002
Published online 4 June 2003 –

Abstract. The effective linear and nonlinear optical properties of metal/dielectric composite media, in which ellipsoidal metal inclusions are distributed in shape, are investigated. The shape distribution function $P(L_x, L_y)$ is assumed to be $2\Delta^{-2}\theta(L_x-1/3+\Delta/3)\theta(L_y-1/3+\Delta/3)\theta(2/3+\Delta/3-L_x-L_y)$, where $\theta(\cdots)$ is the Heaviside function, Δ is the shape variance and L_i are the depolarization factors of the ellipsoidal inclusions along i-symmetric axes ($i = x, y$). Within the spectral representation, we adopt Maxwell-Garnett type approximation to study the effect of shape variance Δ on the effective nonlinear optical properties. Numerical results show that both the effective linear optical absorption $\alpha \sim \omega \mathrm{Im}(\sqrt{\epsilon_e^{(0)}})$ and the modulus of the effective third-order optical nonlinearity enhancement $|\chi_e^{(3)}|/\chi_1^{(3)}$ exhibit the nonmonotonic behavior with Δ. Moreover, with increasing Δ, the optical absorption and the nonlinearity enhancement bands become broad, accompanied with the decrease of their peaks. The adjustment of Δ from 0 to 1 allows us to examine the crossover behavior from no separation to large separation between optical absorption and nonlinearity enhancement peaks. As $\Delta \to 0$, *i.e.*, the ellipsoidal shape deviates slightly from the spherical one, the dependence of $|\chi_e^{(3)}|/\chi_1^{(3)}$ on Δ becomes strong first and then weak with increasing the imaginary part of inclusions' dielectric constant. In the dilute limit, the exact formula for the effective optical nonlinearity is derived, and the present approximation characterizes the exact results better than old mean field one does.

PACS. 42.65.-k Nonlinear optics – 82.70.Dd Colloids – 81.05.Rm Porous materials; granular materials – 72.20.Ht High-field and nonlinear effects

1 Introduction

Nonlinear optical properties of granular composite materials have received much interest because of their potential applications in physics and engineering [1–3]. A typical system for the theoretical and experimental investigations is composed of metallic particles with nonlinear dielectric response, randomly embedded in a dielectric host with linear or nonlinear response. Such a composite system has been found to exhibit strongly optical nonlinearity through the local field and/or geometric resonance effects [4–8].

As in realistic composite systems, the granular inclusions are usually not spherical in shape and even shape distributed, more recently, much work was done in this kind of system, by taking into account the particles' shape [9] and shape distribution [10]. In reference [9], the results show that the effective linear optical absorption and the modulus of the effective third-order optical nonlinearity are strongly dependent on the shape of granular inclusions. However, a large optical nonlinearity enhancement is always accompanied with a large optical absorption. This imperfection places a fundamental constraint on the usefulness of these materials. When the shape distribution of metallic particles is introduced into calculations [10], the separation of the absorption peak from the nonlinearity enhancement one can be realized, and thereby make the figure of merit more attractive.

Previously, for convenience, the shape distribution of inclusions was assumed to distribute uniformly by exhausting all possible ellipsoids [10]. It would be instructive to consider more realistic shape distribution function. In this paper, we will assume the distribution function to be realistic with the form $P(L_x, L_y) = 2\Delta^{-2}\theta(L_x - 1/3 + \Delta/3)\theta(L_y - 1/3 + \Delta/3)\theta(2/3 + \Delta/3 - L_x - L_y)$ [11,12], where $\theta(\cdots)$ is the Heaviside function and the shape variance Δ defines the domain of nonzero value for $P(L_x, L_y)$. Physically, $\Delta = 0$, all granular inclusions are spherical in shape; $\Delta \to 1$, all possible shapes of ellipsoids are

[a] e-mail: lgaophys@pub.sz.jsinfo.net

equiprobable. This kind of distribution form has been applied to investigate the effective absorption and scattering cross section for a system of small non-interacting ellipsoids distributed in shape [11,12]. Theoretically, this form allows us an alternative freedom, *i.e.*, the shape variance, of adjusting the modulus of the optical nonlinearity enhancement. Moreover, such a choice will be useful to examine the crossover behavior from no separation ($\Delta \to 0$) to large separation ($\Delta \to 1$) between the optical absorption and nonlinearity enhancement peaks.

Our investigation is also motivated by recent work [13], in which Goncharenko *et al.* considered the nonlinear optical properties of the composite media in which the granular inclusions are slightly nonspherical (*i.e.* $\Delta \to 0$) and distributed in shape, based on an old mean-field approximation [5]. They found that the role of nonsphericity on the effective optical nonlinearity increases with decreasing the imaginary part of linear dielectric constant of granular inclusions. It is known that the old mean-field approximation adopts the equality $\langle|\mathbf{E}|^2\rangle = |\langle\mathbf{E}^2\rangle|$ ($\langle\cdots\rangle$ represents the spatial average), which is quite rough when the dielectric constants of the components are complex. In present work, we will combine the decoupling approximation [5] with the spectral representation [14,15] to investigate the effective linear dielectric constant and the effective third-order optical nonlinearity. We place special emphasis on the effect of the shape variance Δ on the linear optical absorption and the modulus of the optical nonlinearity enhancement. In order to verify the roughness of the old approximation, numerical results from both the old approximation and the present one will be compared with the exact predictions in the dilute limit.

This paper is organized as follows. In Section 2, we derive the Maxwell-Garnett type approximation by including the shape variance distribution and then obtain the spectral density function analytically. In Section 3, the effect of shape variance Δ on the optical absorption and the optical nonlinearity enhancement is considered. In Section 4, we derive an exact formula for the effective third-order optical nonlinearity of the dilute composite media by assuming the dielectric host to be linear. Then, exact results are in comparison with those obtained from present approximation and the old one adopted by Goncharenko *et al.* [13]. A summary of our results and discussion will be given in Section 5.

2 Maxwell-Garnett type approximation with shape variance distribution

We consider a three-dimensional granular composite, in which ellipsoidal metal particles of the volume fraction f are randomly embedded in an isotropic dielectric medium of the volume fraction $1-f$. The local constitutive electric displacement ($\mathbf{D}$)-electric field ($\mathbf{E}$) relation has the form $\mathbf{D} = \epsilon_i^{(0)}\mathbf{E} + \chi_i^{(3)}|\mathbf{E}|^2\mathbf{E}$, where $\epsilon_i^{(0)}$ and $\chi_i^{(3)}$ are the (scalar) linear dielectric function and third-order nonlinear optical susceptibility of the ith component ($i = 1, 2$). We restrict our discussion within the quasi-static approximation, under which the composite media can be regarded as an homogeneous one, whose effective physical properties are denoted by the effective linear dielectric constant $\epsilon_e^{(0)}$ and effective third-order optical nonlinearity $\chi_e^{(3)}$. As we know, the shape of ellipsoidal particles can be described by three depolarization factors L_x, L_y, and L_z, which satisfy the sum rule $L_x + L_y + L_z = 1$. Thus the distribution function of the depolarization factors is used to indicate the shape distribution of granular inclusions. Here, we assume the distribution function to be [11,12],

$$P(L_x, L_y) = 2\Delta^{-2}\theta\left(L_x - \frac{1}{3} + \frac{\Delta}{3}\right)\theta\left(L_y - \frac{1}{3} + \frac{\Delta}{3}\right) \times \theta\left(-L_x - L_y + \frac{2}{3} + \frac{\Delta}{3}\right), \tag{1}$$

where Δ is the shape variance of the particles, which defines both the domain of nonzero values and the half-width of the $P(L_x, L_y)$ function. Actually, Δ can change from zero (all metal inclusions are spherical in shape) to unity (all possible ellipsoids exist). When the shape distribution is taken into account, the field factor β, defined as the ratio between the local field in metal inclusions and the external applied field, can be obtained from

$$\begin{aligned}\beta &= \frac{2}{3\Delta^2}\int_{\frac{1}{3}(1-\Delta)}^{\frac{1}{3}(1+2\Delta)}\int_{\frac{1}{3}(1-\Delta)}^{\frac{1}{3}(2+\Delta)-L_x}\left[\frac{\epsilon_2^{(0)}}{L_x\epsilon_1^{(0)} + (1-L_x)\epsilon_2^{(0)}} + \frac{\epsilon_2^{(0)}}{L_y\epsilon_1^{(0)} + (1-L_y)\epsilon_2^{(0)}} + \frac{\epsilon_2^{(0)}}{(1-L_x-L_y)\epsilon_1^{(0)} + (L_x+L_y)\epsilon_2^{(0)}}\right]\mathrm{d}L_x\mathrm{d}L_y \\ &= \frac{2}{\Delta^2}s\left[\left(s - \frac{1}{3} - \frac{2}{3}\Delta\right)\ln\left(\frac{s - 1/3 - 2/3\Delta}{s - 1/3 + \Delta/3}\right) + \Delta\right],\end{aligned} \tag{2}$$

where $s \equiv \epsilon_2^{(0)}/(\epsilon_2^{(0)} - \epsilon_1^{(0)})$.

The effective linear dielectric function $\epsilon_e^{(0)}$ has been found to be [10],

$$\epsilon_e^{(0)} = \frac{f\epsilon_1^{(0)}\beta + (1-f)\epsilon_2^{(0)}}{f\beta + (1-f)}. \tag{3}$$

Equation (3) can be indeed valid for non-dilute volume fractions such as $f \leq 0.3$ [16].

Next, we adopt the spectral representation to derive the spectral density function [14,15]. Let $F = 1 - \epsilon_e^{(0)}/\epsilon_2^{(0)}$, one has

$$F(s) = \int_0^1 \frac{m(x)}{s-x}\mathrm{d}x, \tag{4}$$

where the spectral density function $m(x)$ can be obtained through the limiting process,

$$m(x) = -\frac{1}{\pi}\lim_{\eta\to 0^+}\mathrm{Im}\left[F(x + \mathrm{i}\eta)\right]. \tag{5}$$

From equations (3) and (2), $m(x)$ is analytically found to be (after rather bulky calculations),

$$m(x) = \begin{cases} \dfrac{2f(1-f)\Delta^{-2}\,(1/3+2\Delta/3-x)}{De} & \\ \qquad\qquad \text{if} \quad \dfrac{1}{3}-\dfrac{\Delta}{3} \le x \le \dfrac{1}{3}+\dfrac{2\Delta}{3} & (6) \\ 0 \qquad\qquad \text{otherwise} & \end{cases}$$

with

$$De = \left\{2fx\Delta^{-2}\left[\Delta+(x-1/3-2\Delta/3)\right] \times \ln\left[(1/3+2\Delta/3-x)/(x-1/3+\Delta/3)\right]+1-f\right\}^2 + \left[2fx\pi\Delta^{-2}(x-1/3-2\Delta/3)\right]^2.$$

As we have obtained the spectral density function, the effective third-order optical nonlinearity $\chi_e^{(3)}$ can be then evaluated within the mean-field approximation [5],

$$\begin{aligned}\chi_e^{(3)}|\mathbf{E}_0|^2\mathbf{E}_0^2 &= f\chi_1^{(3)}\langle|\mathbf{E}|^2\mathbf{E}^2\rangle_{\mathrm{lin},1}+(1-f)\chi_2^{(3)}\langle|\mathbf{E}|^2\mathbf{E}^2\rangle_{\mathrm{lin},2}\\ &\approx f\chi_1^{(3)}\langle|\mathbf{E}|^2\rangle_{\mathrm{lin},1}\langle\mathbf{E}^2\rangle_{\mathrm{lin},1}\\ &\quad+(1-f)\chi_2^{(3)}\langle|\mathbf{E}|^2\rangle_{\mathrm{lin},2}\langle\mathbf{E}^2\rangle_{\mathrm{lin},2}, \qquad (7)\end{aligned}$$

where the linear local field average $\langle\mathbf{E}^2\rangle_{\mathrm{lin},i}$ and $\langle|\mathbf{E}|^2\rangle_{\mathrm{lin},i}$ are exactly expressed as [6,7],

$$\begin{aligned} f\langle\mathbf{E}^2\rangle_{\mathrm{lin},1} &= \int_0^1 \frac{s^2m(x)}{(s-x)^2}\mathrm{d}x\mathbf{E}_0^2\\ (1-f)\langle\mathbf{E}^2\rangle_{\mathrm{lin},2} &= \left[1-\int_0^1 \frac{(s^2-x)m(x)}{(s-x)^2}\mathrm{d}x\right]\mathbf{E}_0^2, \qquad (8)\end{aligned}$$

and

$$\begin{aligned} f\langle|\mathbf{E}|^2\rangle_{\mathrm{lin},1} &= \int_0^1 \frac{|s|^2m(x)}{|s-x|^2}\mathrm{d}x|\mathbf{E}_0|^2\\ (1-f)\langle|\mathbf{E}|^2\rangle_{\mathrm{lin},2} &= \left[1-\int_0^1 \frac{(|s|^2-x)m(x)}{|s-x|^2}\mathrm{d}x\right]|\mathbf{E}_0|^2. \qquad (9)\end{aligned}$$

In equation (7), the decoupling treatment has been adopted, which works well when the local field in the granular inclusions is fairly uniform.

So far, we have formulated our present approximation based on equation (3), equations (6–9), to calculate the effective linear dielectric constant $\epsilon_e^{(0)}$ and the effective third-order optical nonlinearity $\chi_e^{(3)}$.

It is known that, without any knowledge of the spectral information, $\langle\mathbf{E}^2\rangle_{\mathrm{lin},i}$ in equation (7) can also be expressed as [5],

$$\langle\mathbf{E}^2\rangle_{\mathrm{lin},1} = \frac{1}{f}\frac{\partial\epsilon_e^{(0)}}{\partial\epsilon_1^{(0)}}\mathbf{E}_0^2 \quad\text{and}\quad \langle\mathbf{E}^2\rangle_{\mathrm{lin},2} = \frac{1}{1-f}\frac{\partial\epsilon_e^{(0)}}{\partial\epsilon_2^{(0)}}\mathbf{E}_0^2. \qquad (10)$$

For the other term $\langle|\mathbf{E}|^2\rangle_{\mathrm{lin},i}$ in equation (7), Goncharenko *et al.* [13] admits the approximate relation,

$$\langle|\mathbf{E}|^2\rangle_{\mathrm{lin},1} \approx |\langle\mathbf{E}^2\rangle_{\mathrm{lin},1}| = \frac{1}{f}\left|\frac{\partial\epsilon_e^{(0)}}{\partial\epsilon_1^{(0)}}\right||\mathbf{E}_0|^2 \qquad (11)$$

and

$$\langle|\mathbf{E}|^2\rangle_{\mathrm{lin},2} \approx |\langle\mathbf{E}^2\rangle_{\mathrm{lin},2}| = \frac{1}{1-f}\left|\frac{\partial\epsilon_e^{(0)}}{\partial\epsilon_2^{(0)}}\right||\mathbf{E}_0|^2. \qquad (12)$$

As can be seen from equations (8) and (9), above approximations become exact only when $\epsilon_i^{(0)}$ takes real value and are very rough when the local field is complex (resulting from the complex dielectric function of the metal component).

Introducing equations (10–12) into equation (7), we then have a rough approximation for $\chi_e^{(3)}$,

$$\chi_e^{(3)} = \frac{\chi_1^{(3)}}{f}\left|\frac{\partial\epsilon_e^{(0)}}{\partial\epsilon_1^{(0)}}\right|\frac{\partial\epsilon_e^{(0)}}{\partial\epsilon_1^{(0)}} + \frac{\chi_2^{(3)}}{1-f}\left|\frac{\partial\epsilon_e^{(0)}}{\partial\epsilon_2^{(0)}}\right|\frac{\partial\epsilon_e^{(0)}}{\partial\epsilon_2^{(0)}}. \qquad (13)$$

3 Optical absorption, optical nonlinearity and figure of merit

As numerical illustration, the linear dielectric function of metal particles is assumed to be Drude-like with the form,

$$\epsilon_1^{(0)}(\omega) = 1 - \frac{\omega_p^2}{\omega(\omega+\mathrm{i}\gamma)} \qquad (14)$$

where ω_p denotes the bulk plasmon frequency and γ is the damping constant. Although our method is valid for both metal and dielectric components being nonlinear, without loss of generality, we neglect the optical nonlinearity of the dielectric host by letting $\chi_2^{(3)}=0$, according to recent observations in experiments on metal/dielectric composites [17].

In Figure 1, we plot the linear optical absorption coefficient $\alpha \sim \mathrm{Im}[\sqrt{\epsilon_e^{(0)}}]\omega/\omega_p$ against the incident frequency ω/ω_p for various Δ and f. It is evident that the shape variance Δ plays an important role in determining both the linear optical absorption peak and the surface plasmon resonant band. With increasing Δ, the linear absorption peak decreases monotonically, while the resonant band becomes broad, as expected. When $\Delta \to 1$, the results naturally reduce to those in reference [10]. As far as the effect of f is concerned, with increasing f, the absorption peak increases, but its position is not shifted obviously.

In Figure 2, the modulus of the optical nonlinearity enhancement $|\chi_e^{(3)}|/\chi_1^{(3)}$ is shown as a function of ω/ω_p. With increasing Δ, $|\chi_e^{(3)}|/\chi_1^{(3)}$ exhibits similar behavior as optical absorption does, *i.e.*, the optical nonlinearity peak decreases accompanied with broad enhancement spectra. As previous work assumed the granular inclusions to be

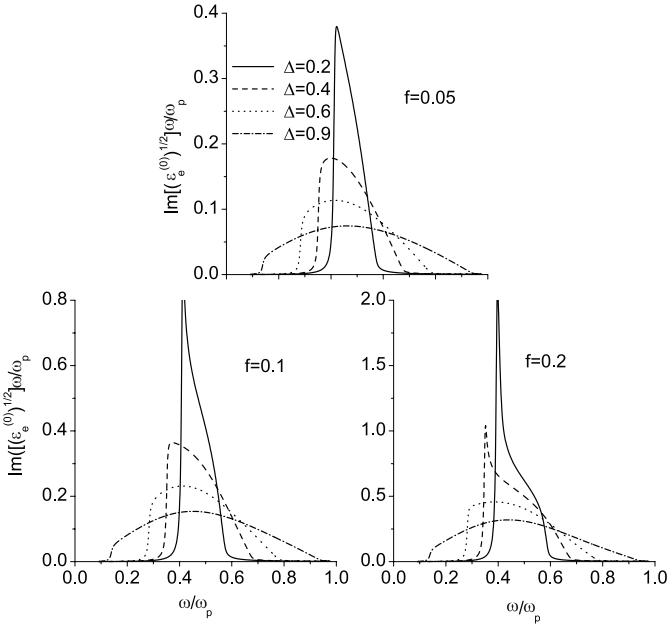

Fig. 1. The linear optical absorption $\alpha \sim \mathrm{Im}[\sqrt{\epsilon_e^{(0)}}]\omega/\omega_p$ against the incident frequency ω/ω_p for various f and Δ.

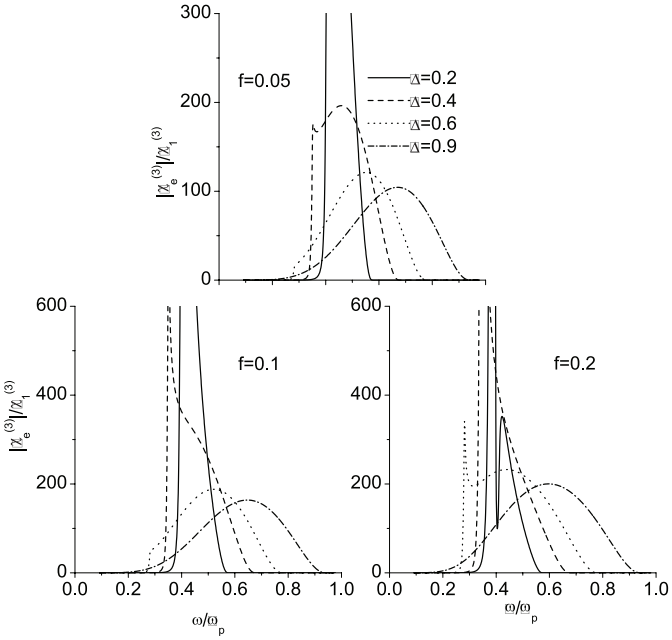

Fig. 2. The modulus of the optical nonlinearity enhancement $|\chi_e^{(3)}|/\chi_1^{(3)}$ against ω/ω_p for various f and Δ.

spherical, the prediction of original Maxwell-Garnett approximation ($\Delta = 0$) [7] yields at least two orders larger than experimental reports [18]. Here, we believe that in order to reduce the discrepancies between theoretical and experimental results, the shape distribution of granular inclusions should be considered. Moreover, as the shape variance is increased, we also predict that the nonlinearity enhancement peak shifts to long wavelengths first and then back to short wavelengths.

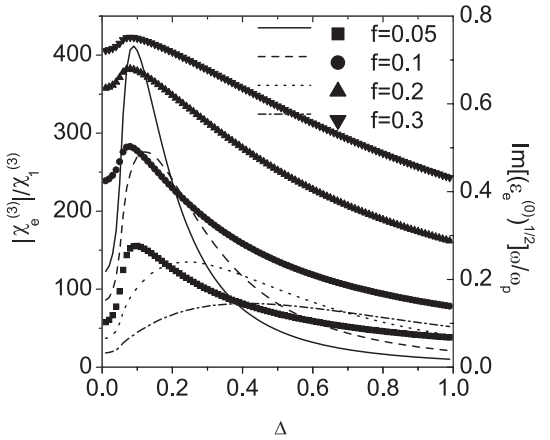

Fig. 3. $|\chi_e^{(3)}|/\chi_1^{(3)}$ (lines) and $\alpha \sim \mathrm{Im}\left[\sqrt{\epsilon_e^{(0)}}\right]\omega/\omega_p$ (symbols) against Δ for $\omega/\omega_p = 0.5$ and various f.

In order to show clearly the shape variance effect, we also plot α and $|\chi_e^{(3)}|/\chi_1^{(3)}$ as a function of Δ for given ω/ω_p and various f in Figure 3. Both the optical absorption and nonlinearity enhancement are observed to exhibit nonmonotonic behavior as Δ is increased, *i.e.*, they increase initially at small Δ, go through maxima at optimal Δ, then decrease with further increasing Δ. Thus, for a certain incident frequency, the adjustment of the shape variance provides an alternative way to achieve large modulus of the optical nonlinearity enhancement. In addition, with increasing f, on the one hand, the optical absorption peak increases, but the nonlinearity enhancement peak decreases; on the other hand, the position of optical absorption peak is almost independent of f, whereas that of optical nonlinearity one is shifted to large Δ significantly.

For practical applications, the most useful parameter is the figure of merit (FOM), defined as the ratio between $|\chi_e^{(3)}|/\chi_1^{(3)}$ and α. Figure 4 shows FOM as a function of ω/ω_p for various values of Δ and f. As Δ is small, FOM is quite large in the middle-frequency region around $\omega \approx 0.4\omega_p$; at the same time, large optical absorption is also observed, limiting the potential applications in this frequency region. When Δ is large and tends to 1, in the high-frequency region, FOM is still large, but the small optical absorption is achieved. Moreover, the larger Δ, the broader the resonant bands of FOM become. Due to these properties, introducing the shape distribution with large Δ in this frequency region is beneficial to enhance the FOM, and thereby increases the applicability of this kind of composite media.

The separation of the nonlinearity enhancement peak from the absorption one has been observed in the metal/dielectric composites with an assumption that all possible ellipsoidal particles are distributed uniformly [10]. In present work, the shape variance Δ allows us to examine the crossover behavior from no separation ($\Delta \to 0$) to large separation ($\Delta \to 1$) between optical absorption

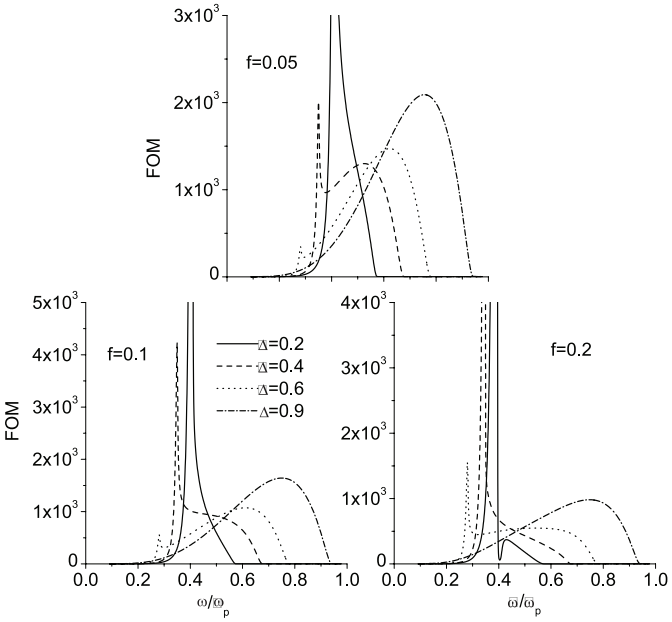

Fig. 4. The figure of merit (FOM $\equiv |\chi_e^{(3)}|/\chi_1^{(3)}/\alpha$) against ω/ω_p for various Δ and f.

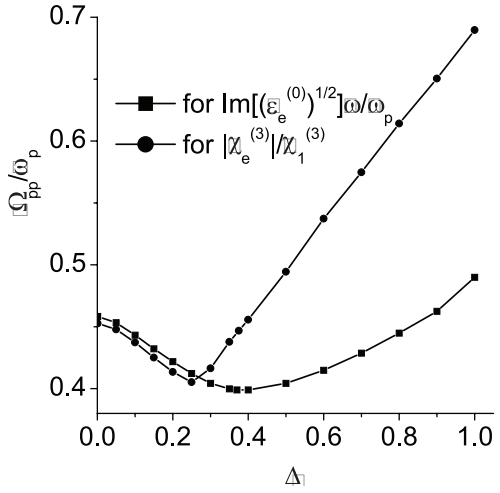

Fig. 5. Positions of optical nonlinearity enhancement peak and linear optical absorption peak Ω_{pp} against Δ for $f = 0.05$. Note that large separation is found for large Δ.

peak and optical nonlinearity enhancement one, as shown in Figure 5. In Figure 5, we plot the positions of both optical absorption and nonlinearity enhancement peaks Ω_{pp} against Δ for $f = 0.05$. When Δ is small, two positions are quite close (strictly speaking, the position of optical absorption peak is slightly larger than that of nonlinearity enhancement peak); with increasing Δ, both of them exhibit red-shifted first and then blue-shifted, leading to the existence of a point of intersection at $\Delta \approx 0.27$; when $\Delta > 0.27$, the position of optical nonlinearity enhancement peak increases rapidly and the separation of two positions becomes more and more distinct with further

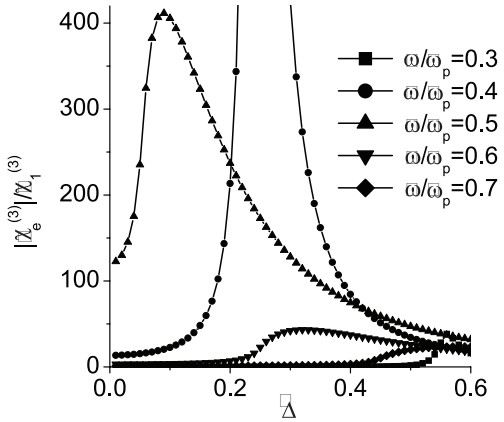

Fig. 6. $|\chi_e^{(3)}|/\chi_1^{(3)}$ against small Δ for $f = 0.05$ and various ω/ω_p.

increasing Δ. Such crossover behavior is new and cannot be predicted in our previous work [10].

We also plot the modulus of the optical nonlinearity enhancement $|\chi_e^{(3)}|/\chi_1^{(3)}$ as a function of small Δ (*i.e.*, the shape of granular inclusions deviates slightly from the spherical one) for $f = 0.05$ and various ω/ω_p in Figure 6. For $\omega = 0.3\omega_p$, $|\chi_e^{(3)}|/\chi_1^{(3)}$ is almost independent of Δ; with increasing ω/ω_p, the dependence of $|\chi_e^{(3)}|/\chi_1^{(3)}$ on Δ becomes significant (for example, for $\omega = 0.5\omega_p$, $|\chi_e^{(3)}|/\chi_1^{(3)}$ increases rapidly with small Δ); further increasing ω leads to weak dependence of $|\chi_e^{(3)}|/\chi_1^{(3)}$ on Δ again. According to equation (14), the increase of the incident frequency means the decrease of $\mathrm{Im}(\epsilon_1^{(0)})$. Thus, we conclude that the role of nonsphericity ($\Delta \to 0$) increases first and then decreases with increasing ω/ω_p [or decreasing $\mathrm{Im}(\epsilon_1^{(0)})$], in contrast to the previous report [13].

4 Effective optical nonlinearity in the dilute limit

It is well known that the present approximation is exact for spherical inclusions ($\Delta = 0$). However, for randomly oriented ellipsoidal granular inclusions, the decoupling treatment $\langle |\mathbf{E}|^2 \mathbf{E}^2 \rangle_{\mathrm{lin},i} = \langle |\mathbf{E}|^2 \rangle_{\mathrm{lin},i} \langle \mathbf{E}^2 \rangle_{\mathrm{lin},i}$ becomes rough even in the dilute limit. Here, the mean fourth power of the linear local electric field within the randomly oriented ellipsoidal particles with dilute volume fractions is calculated according to the rule,

$$\langle f(\theta,\phi) \rangle = \frac{\int_0^{2\pi} \int_0^{\pi} f(\theta,\phi) \sin\theta \mathrm{d}\theta \mathrm{d}\phi}{\int_0^{2\pi} \int_0^{\pi} \sin\theta \mathrm{d}\theta \mathrm{d}\phi}, \tag{15}$$

and is readily found to be

$$\frac{\langle |\mathbf{E}|^2 \mathbf{E}^2 \rangle_{\mathrm{lin},1}}{|\mathbf{E}_0|^2 \mathbf{E}_0^2} = \frac{1}{15} \Big[(3\beta_x^2 + \beta_y^2 + \beta_z^2) |\beta_x|^2 + (\beta_x^2 + 3\beta_y^2 + \beta_z^2) |\beta_y|^2 + (\beta_x^2 + \beta_y^2 + 3\beta_z^2) |\beta_z|^2 \Big], \tag{16}$$

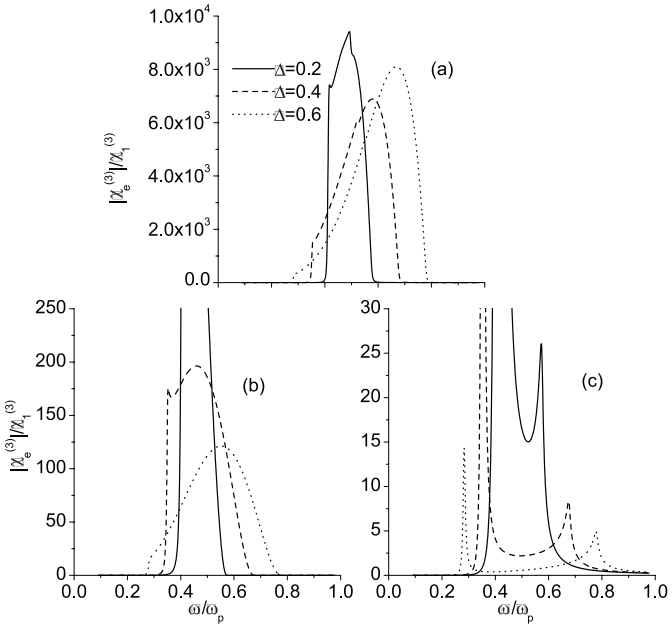

Fig. 7. $|\chi_e^{(3)}|/\chi_1^{(3)}$ against ω/ω_p in the dilute limit $f = 0.05$. We show: (a) the exact results from equation (16), (b) the present approximation from equations (6–9) and (c) the old approximation from equation (13).

where $\beta_j = \epsilon_2^{(0)}/[L_j\epsilon_1^{(0)} + (1 - L_j)\epsilon_2^{(0)}]$ $(j = x, y, z)$. If we choose $\chi_2^{(3)}$ to be zero, from symmetry considerations, the effective optical nonlinearity of the composites with a shape variance distribution can be expressed as:

$$\chi_e^{(3)} = f\chi_1^{(3)} \int\int P(L_x, L_y) \frac{\langle |\mathbf{E}|^2 \mathbf{E}^2 \rangle_{\mathrm{lin},i}}{|\mathbf{E}_0|^2 \mathbf{E}_0^2} \mathrm{d}L_x \mathrm{d}L_y$$

$$= \frac{2f\chi_1^{(3)}}{5\Delta^2} \int_{\frac{1}{3}(1-\Delta)}^{\frac{1}{3}(1+2\Delta)} \int_{\frac{1}{3}(1-\Delta)}^{\frac{1}{3}(2+\Delta)-L_x} \left(3\beta_x^2 + \beta_y^2 + \beta_z^2\right)$$

$$\times |\beta_x|^2 \mathrm{d}L_x \mathrm{d}L_y. \quad (17)$$

Equation (17) is an exact formula for the effective optical nonlinearity of composites in which nonlinear ellipsoidal metal inclusions with shape distribution described by equation (1) are randomly embedded in the linear dielectric host in the dilute limit.

In Figure 7, we plot $|\chi_e^{(3)}|/\chi_1^{(3)}$ *versus* ω/ω_p in the dilute limit calculated from equation (17). For comparison, we also show the results from our approximation equations (6–9) and the old one equation (13). Our approximation characterizes the exact results well, except that there are some discrepancies in the orders of magnitude, due to the mean-field approximation adopted. With the old approximation equation (13), the most drastic features are two enhancement peaks at frequencies around the surface plasmon band edges, which are quite different from the exact predictions. Moreover, both our approximation and the old one underestimate the exact results, but the old approximation underestimates them more than our approximation does. Such a conclusion results from the fact that in equation (13), $|\langle \mathbf{E}^2 \rangle_{\mathrm{lin},i}|$, which enters into the old approximation is always less than $\langle |\mathbf{E}|^2 \rangle_{\mathrm{lin},i}$, when the dielectric loss becomes important. Qualitatively, $|\langle \mathbf{E}^2 \rangle_{\mathrm{lin},i}|$ can, in principle, be zero for appropriate conditions, while $\langle |\mathbf{E}|^2 \rangle_{\mathrm{lin},i}$ can never be zero.

5 Discussion and conclusions

In this paper, we have adopted the Maxwell-Garnett type approximation to study the effective linear and nonlinear optical properties of the metal-dielectric composites with the shape variance distribution with the spectral representation method. By introducing the shape variance distribution Δ of granular particles, we get the knowledge that with the increase of Δ, both the optical absorption and optical nonlinearity enhancement peaks decrease, and their surface plasmon bands become broad. By suitable adjustment of the shape variance, we are able to achieve large modulus of the optical nonlinearity enhancement in some frequency region. Moreover, it allows us to examine the crossover behavior from no separation to large separation between two optical resonant peaks. Thus we conclude, we can realize the separation of the optical absorption and optical nonlinearity peaks for large Δ and achieve the optimal figure of merit in high frequency region. When the granular inclusions are slightly nonspherical, the role of nonsphericity on the optical nonlinearity enhancement increases and then decreases with decreasing $\mathrm{Im}(\epsilon_1^{(0)})$. By comparing our approximation with the old one, we find that present approximation characterizes qualitatively the exact results in the dilute limit.

We derive the Maxwell-Garnett type approximation for asymmetric composites in which the volume fractions of granular inclusions cannot be very large. Based on the condition of zero average dipole moment, Bruggeman-type effective medium approximation with shape distributions for symmetric microstructures can be derived [19]. In this connection, both collective phenomena and percolation effect will take place. Preliminary results show that the percolation threshold will be dependent on the shape variance Δ. Thus, the percolation network can be formed by adjusting the shape distribution of the nonlinear component. Near the percolation threshold, it would be interesting to study the critical behavior of the modulus of the optical nonlinearity enhancement in the composite media with shape distribution. This work is in progress and will be reported elsewhere.

This work was supported by the National Natural Science Foundation of China for financial support under Grant No.10204017 and by the Natural Science of Jiangsu Province for financial support under Grant No. BK2002038. L.G. acknowledges Prof. Z.Y. Li and K.W. Yu for useful discussions.

References

1. C. Flytzanis, F. Hache, M.C. Klein, D. Ricard, P. Roussignol, Prog. Opt. **29**, 323 (1991)
2. D.J. Bergman, D. Stroud, Sol. State Phys. **46**, edited by H. Ehrenreich, D. Turnbull (Academic Press, New York, 1992)
3. A.K. Sarychev, V.M. Shalaev, Phys. Rep. **335**, 275 (2000)
4. G.S. Agarwal, S.D. Gupta, Phys. Rev. A **38**, 5678 (1988)
5. D. Stroud, V.E. Wood, J. Opt. Soc. Am. B **6**, 778 (1989)
6. K.P. Yuen, M.F. Law, K.W. Yu, Ping Sheng, Phys. Rev. E **56**, R1322 (1997)
7. H.R. Ma, R.F. Xiao, Ping Sheng, J. Opt. Soc. Am. B **15**, 1022 (1998)
8. L. Gao, Z.Y. Li, J. Appl. Phys. **87**, 1620 (2000)
9. L. Gao, J.T.K. Wan, K.W. Yu, Z.Y. Li, J. Phys. Cond. Matt. **12**, 6825 (2000)
10. L. Gao, K.W. Yu, Z.Y. Li, Bambi Hu, Phys. Rev. E **64**, 036615 (2001)
11. A.V. Goncharenko, E.F. Venger, S.N. Zavadskii, J. Opt. Soc. Am. B **13**, 2392 (1996)
12. A.V. Goncharenko, Y.G. Semenov, E.F. Venger, J. Opt. Soc. Am. A **16**, 517 (1999)
13. A.V. Goncharenko, V.V. Popelnukh, E.F. Venger, J. Phys. D: Appl. Phys. **35**, 1833 (2002)
14. D.J. Bergman, Phys. Rep. **43**, 377 (1978)
15. G.W.Milton, J. Appl. Phys. **52**, 5286 (1981)
16. C.W. Nan, R. Birringer, D.R. Clarke, H. Gleiter, J. Appl. Phys. **81**, 6692 (1997)
17. H.B. Liao, R.F. Xiao, J.S. Fu, G.K.L. Wong, Appl. Phys. B **65**, 673 (1997)
18. H.B. Liao, R.F. Xiao, J.S. Fu, P. Yu, G.K.L. Wong, Ping Sheng, Appl. Phys. Lett. **70**, 1 (1997)
19. D. Stroud, Phys. Rev. B **19**, 1783 (1979)